Postprint of: Singh G., Kumar R., Mikielewicz D., Effect of Flow Normalization in Micro-Pin-Finned Heat Sink: Numerical Study, JOURNAL OF THERMOPHYSICS AND HEAT TRANSFER, DOI: 10.2514/1.T6011

Effect of Flow Normalization in Micro Pin Finned Heat Sink: Numerical Study

Gurjeet Singh,[1] Ritunesh Kumar,[2]
Department of Mechanical Engineering, Indian Institute of Technology Indore, Khandwa Road, Simrol, India-453552

and
Dariusz Mikielewicz[3]
Gdansk University of Technology, Faculty of Mechanical Engineering, ul.Narutowicza 11/12, 80-233 Gdansk, Poland

Micro pin fin heat sink (MPFHS) is widely employed for the heat transfer enhancement of microchannel heat sinks (MCHSs). In the current paper the effect of flow normalization on the thermo-hydraulic performance of micro pin finned heat sinks (MPFHSs) is studied numerically. Two geometries of MPFHSs; conventional design micro pin fin heat sink (CD-MPFHS) with uniform width micro pin fin and proposed design micro pin fin heat sink (PD-MPFHS) with non-uniform width micro pin fin are studied. Flow distribution analysis in the primary and secondary channels of MPFHSs is carried out. More flow resistance offered by wider central micro pin fins diverts more flow towards side channels. As a result of which better flow distribution in primary channels and higher flow across secondary channels is noticed for PD-MPFHS as compared to CD-MPFHS. As a result of that maximum and average base temperatures are reduced by 4.6 K and 2.2 K as compared to CD-MPFHS. Nusselt number increased by 10.1% and better thermal-hydraulic performance index has been offered by the PD-MPFHS for entire studied Reynolds number range.

Nomenclature

[1] Research Scholar, Department of Mechanical Engineering, Madhya Pradesh, India.
[2] Associate Professor, Department of Mechanical Engineering, Madhya Pradesh, India, ritunesh@iiti.ac.in (Corresponding Author).
[3] Professor, Faculty of Mechanical Engineering, Gdansk, Poland.

Ch	=	primary channel
c_p	=	specific heat (J/kg k)
CD	=	conventional design
Ch	=	primary channels
D_h	=	hydraulic diameter of channel (m)
e	=	fin number
f	=	friction factor
H	=	height (m)
i	=	channel number
k	=	thermal conductivity (W/m K)
L	=	length (m)
$\dot{m}$	=	mass flow rate (kg/s)
MFR	=	mass flow rate (kg/s)
N	=	pin fins rows along the flow length
NMFR	=	normalized mass flow rate (kg/ kg)
Nu	=	Nusselt number
Nu_{fin}	=	Nusselt number based on fin hydraulic diameter
ΔP	=	pressure drop (Pa)
PD	=	proposed design
MPFHS	=	micro pin fin heat sink
Pr	=	Prandtl number
q''	=	heat flux (W/m^2)
Re_{avg}	=	Reynolds number based average velocity through channel
Re_{fin}	=	Reynolds number based on fin hydraulic diameter
Re_{in}	=	Reynolds number at the inlet of heat sink
Sec	=	Secondary channel
T	=	temperature (K)
$\boldsymbol{V}$	=	velocity vector (m/s)

v	=	velocity (m/s)
V_f	=	volume of fluid in channels (m^3)
W	=	width (m)
x	=	x-coordinate (transverse direction)
y	=	y-coordinate (longitudinal direction)

Greek Symbols

ε	=	absolute percentage deviation
μ	=	viscosity (kg/m s)
ϕ	=	maldistribution factor
η	=	thermal-hydraulic performance index
ρ	=	density (kg/m^3)
Γ	=	interface

Subscripts

b	=	base of microchannels projected area
avg	=	average
ch	=	primary channel
f	=	fluid
HS	=	heat sink
i	=	channel number
j	=	iteration number
e	=	fin number
M	=	manifold
max	=	maximum
min	=	minimum
ND	=	non dimensional
s	=	solid
sec	=	secondary channel

vavg = volumetric average

x1 = inlet of the secondary channel

x2 = outlet of the secondary channel

y1 = inlet of the primary channel

y2 = outlet of the secondary channel

I. Introduction

EFFICIENT thermal management is accepted as the biggest hurdle, which may decelerate the future development of high performance computers and data centers. The unadorned longings for high speed computing, better functionality and size miniaturization have fired an extraordinary surge in the chip heat dissipation requirement. Selection of appropriate cooling technique is mandatory for ensuring high reliability and avoiding premature failure of microprocessor of the system. Air cooling methods are no longer adequate to satisfy the heat dissipation demands of modern age CPUs, and in this regard, liquid cooling has become undisputed cooling option for high speed computers and datacenters [1-3]. Among the liquid cooling – microchannel heat sink (MCHS) is the most efficient way of dissipating large amount of heat from the tiny base area of high-end microprocessors. MCHS is basically a cooling plate on whose surface full sized (inlet to outlet plenum) microfins are cut at regular intervals to form micro sized channels between them. It offers extremely high heat transfer coefficient even at very low coolant flow rate. MCHSs cooling technology had received increased attention since the pioneer work of Tuckerman and Pease [4]. And, at present it is one of most widely explored area of research in heat transfer. Apart of conventional heat transfer applications such as microprocessor cooling [5], refrigeration and air-conditioning [6], gas turbine [7], aerospace [8] and laser diode cooling [9], the microchannels are engrossed in other fields also including medical [10], biology [11] and chemical reactors [12]. Two-phase flow boiling in microchannel enjoy manifold higher heat transfer performance than the conforming single phase heat transfer, but due to various associated instabilities, it is less preferable for applications demanding consistent performance of the heat sink. Qu and Mudawar [13] verified the applicability of Navier-Stokes and energy balance equations for the single phase flow in microchannels by validating their experimental observations with the numerical results and opened pathways for the dedicated numerical studies. A lot of experimental and numerical studies had been carried out on the single phase flow in microchannels in the past two decades [14-19]. Various active (vibrations [20], flow pulsations and synthetic jets

[21, 22], etc.) and passive (extended surfaces [23, 24], double layered microchannels [25], ribs and cavities [26, 27], wavy microchannels [28], microchambers [29], vortex generators [30], nanofluid and porous media [31, 32] heat transfer enhancement techniques had been explored for boosting the performance of single phase heat transfer in MCHS. The presence of a significant temperature non-uniformity across parallel channels and along the flow direction are the two main limitations of the single phase flow in MCHS. The temperature variation in the flow direction is the fundamental nature of single phase flow, temperature variation across the parallel microchannels mainly arises due to maldistribution of flow as well as adiabatic/free convection side boundary conditions. Normalization of the surface temperature non-uniformity is desirable to avoid hot-spots generation, which is the major reason responsible for failure of ICs in microprocessor [33] and it is also expected to help in improving the performance of heat transfer process.

Kishimotto and Sasaki [34] were the first to propose the concept of micro pin fin heat sink (diamond shaped) to avoid the excessive heating of substrate temperature. Through their analytical study they claimed 25% reduction in substrate temperature as compared to conventional channel design. Steinke and Kandlikar [35] suggested the concept of secondary flow for fluid mixing between parallel channels of MCHS. They proposed two potential methods to generate secondary flow between channels: through interconnecting oblique or venturi shaped secondary channels. Experimental investigation on micro pin finned heat sink (MPFHS) was started by Peles group [36, 37], alluding the miniaturization of regular macro scaled pin fin heat sink. Kosar et al. [36] experimentally investigated pressure drop/friction factor for inline and staggered arrangement of micro pin fins of circular and diamond shape. Highest pressure drop was noticed for diamond shaped staggered arrangement. They proposed new correlation including end wall and fin density effect for accurate prediction of pressure drop for MPFHS. Peles et al. [37] developed (through analytical results) simplified expression for the estimation of total thermal resistance of MPFHS and validated it with pertinent experiments. They also concluded that thermal-hydraulic performance of the MPFHS is superior to plain MCHS. Kosar and Peles [38] proposed correlations for the prediction of Nusselt number following conventional form of it ($Nu_{\mathrm{avg}} = c1\, Re_{\mathrm{avg}}^{\mathrm{c2}} Pr_{\mathrm{avg}}^{\mathrm{c3}}$) and correction factor $\left(\frac{Pr_{\mathrm{f,avg}}}{Pr_{\mathrm{s,avg}}}\right)^{\mathrm{c4}}$ for MPFHS (where, c1, c2, c3 and c4 are constants). Furthermore, effect of different geometric parameters of micro pin fins (shape, arrangement and spacing) had been systematically investigated by many authors including the pioneering efforts by Peles group [39]. Qu and Shi-Ho [40] experimentally investigated staggered square MPFHS. They noticed that existing micro pin fin correlation by [38] over predicted their experimental observation, they suggested new

coefficients for constants: c1, c2 and c3 for accurate prediction of Nusselt number. Lee et al. [41] proposed the concept of oblique fins by breaking continuous MCHS fins into oblique sections. Their numerical study showed that significant enhancement in the local and global heat transfer coefficient (~80%) can be achieved by the oblique MPFHS in comparison to conventional MCHS at negligible pressure drop penalty. John et al. [42] compared the performance of inline circular and square MPFHS. They reported better performance for the circular micro pin fins at low Reynolds number (Re < 300) and for the square micro fin pins at higher Reynolds number. Hasan [43] numerically compared the heat transfer and pressure drop of different micro pin fin (square, circle and triangle) heat sinks of staggered arrangement. They reported best heat transfer performance for circular pin fins and highest pressure drop for square pin fins. Duangthongsuk and Wongwises [44] experimentally compared the thermal and hydraulic performance of circular and square MPFHSs. They reported better heat transfer and lower pressure drop for circular pin fin design. Mou et al. [45] numerically investigated the fluid flow distribution effect on the heat transfer performance of oblique finned MCHS. They noticed non uniform fluid flow distribution and secondary flow migration in oblique finned MCHS. They further reported that fluid flow migration did not influence significantly the flow distribution in channels lying in the dimensionless width zone of range ($0.2 < W_{ND} < 0.8$). Mohammadi and Kosar [46, 47] studied the thermal and hydraulic performance of circular MPFHS for inline [46] and staggered [47] arrangements. They noticed higher pressure drop and Nusselt number for staggered arrangement of micro pin fins. They also reported lower thermal-hydraulic performance index for staggered arranged of pin fins due to associated higher pressure drops. Xu and Wu [48] performed an experimental study to examine the heat transfer and pressure drop characteristics of micro pin fins of different shapes (circle, square, diamond and ellipse), arrangements (inline/staggered) and design parameters. They noticed lowest average thermal resistance for staggered diamond micro pin fins. Whereas, higher thermal-hydraulic performance is noticed for staggered elliptical micro pin fins due to lower pressure drop as compared to staggered arrangements of other pin fin shapes. New correlations for Nusselt number and friction factor are proposed for different shapes of micro pin fins.

It can be concluded from the above literature survey that most of the past studies on the MPFHS had been carried out either for a single channel [41, 42] or for a complete heat sink by considering uniform flow distribution [43, 45-47]. The above procedures are technically not correct as they cannot replicate the fluid flow behavior through the secondary channels on account of significant flow non-uniformity at the inlet of micro pin fins. Few advance configurations (staggered or oblique fins arrangements) facilitate in improving the thermal performance of

the micro pin fin heat sink but at the cost of very high pressure drop penalty [47]. Hence, maturing the inline micro pin fin arrangement is expected to bring more fruitful outcomes. In the current study the efforts had been made to study the influence of fluid flow non-uniformity on the performance of MPFHS, it is well studied for the MCHS by many past researchers [49-56]. But, no effort has been made yet to study the effect of flow non-uniformity in MPFHS. Hence, the current numerical study is dedicated to investigate the effect of flow maldistribution in inline MPFHS. Detailed analysis of fluid flow distribution in primary and secondary channels as well as heat transfer analysis of MPFHS is carried out.

II. Problem Description and Numerical Model

A. Geometry Description

In the recent study of present authors [54], a new design MCHS (variable width parallel microchannels) had been proposed for the mitigation of flow non-uniformity in parallel microchannels of the heat sink. The dimension of individual parallel microchannels in the proposed design is calculated by Eq. (1), following an iterative procedure given in detail by [54]. Figures 1(a) and 1(c) show the geometries of conventional design microchannel heat sink (CD-MCHS) and proposed design microchannel heat sink (PD-MCHS) respectively. Due to the symmetry of current design only half geometry is considered for the numerical analysis.

$$1 - NMFR_{\mathrm{ch,i}}\big|_{\mathrm{j}} = \frac{W_{\mathrm{ch,i}}\big|_{j+1} - W_{\mathrm{ch,i}}\big|_{\mathrm{j}}}{W_{\mathrm{ch,i}}\big|_{\mathrm{j+1}}} \quad (1)$$

Where, $NMFR_{\mathrm{ch,i}}\big|_{\mathrm{j}} = \frac{\dot{m}_{\mathrm{i}}|_{\mathrm{j}}}{\dot{m}_{\mathrm{avg}}}$

In the current study a conventional design micro pin finned heat sink (CD-MPFHS) is generated by creating uniform secondary channels in geometry of the CD-MCHS as shown in Fig. 1(b). In order to access the benefits of variable width approach in MPFHS; the geometry of PD-MCHS is converted to proposed design micro pin finned heat sink (PD-MPFHS) in the similar manner (by creating uniform secondary channels) as shown in Fig. 1(d). Dimensions of all designs are same as given in Table 1. Width of cut for secondary channels (W_{sec}) is kept constant as 0.26 mm for both designs of MPFHS (CD-MPFHS and PD-MPFHS). Thus, resulted design of CD-MPFHS and PD-MPFHS consists of 25 primary channels and 19 secondary channels. In order to remove the non-uniformity across the inlet and outlet manifold, micro pin fin of length 0.19 mm are provided at start and end of finned area (for

N=1 and 20 in Fig. 1(d)). Width of individual primary channels (W_{ch}) and fin width (W_{fin}) for PD-MPFHS are given in Table 2. Dimensions of the inlet/outlet manifolds are fixed for both designs.

B. Numerical Modeling

Generalized mass, momentum and energy equations are considered to capture the fluid flow and heat transfer characteristics of single phase liquid flow in MCHS. Following assumptions are made for the current numerical analysis:

1) Flow is assumed to be steady, laminar and Newtonian.
2) Effect of the body and surface tension forces is neglected.
3) Radiation and natural convectional effects are neglected.

Following above assumptions, the basic governing equations for the fluid part are Eqs. (2)-(4).

$$\nabla.(\rho_f \boldsymbol{V}) = 0 \tag{2}$$

$$\nabla.(\rho_f \boldsymbol{V}\boldsymbol{V}) = -\nabla P + \nabla.\mu_f[(\nabla \boldsymbol{V} + \nabla \boldsymbol{V}^t) - 2/3\,\nabla.\boldsymbol{V}] \tag{3}$$

$$\nabla.\left(\rho_f c_p \boldsymbol{V} T\right) = -\nabla.(k_f \nabla T) \tag{4}$$

Similarly, for the solid part the governing energy balance equation is Eq. (5).

$$k_s \nabla^2 T = 0 \tag{5}$$

The copper substrate is assumed to have constant thermo-physical properties (k_s = 401 W/m K, ρ_s = 8978 kg/m^3, and c_{ps} = 381 J/kg K) whereas, for the working media (water) variable thermo-physical properties are taken (https://syeilendrapramuditya.wordpress.com/2011/08/20/water-thermodynamic-properties/).

Above governing equations are solved by assuming uniform velocity and temperature characteristics at the inlet of MCHS. Velocity values are varied in the range of 1.35-2.69 m/s which correspond to inlet Reynolds number of 800-1600 and inlet temperature is set as 288.15 K. At the outlet of the MCHS constant atmospheric condition is assumed. Solid and fluid surfaces are coupled at the interface by assuming: $\boldsymbol{V} = 0$ (No slip), $T_s = T_f$, and $-k_s\left(\frac{\partial T_s}{\partial \eta}\right) = -k_f\left(\frac{\partial T_f}{\partial \eta}\right)$. A fixed heat flux of 100 W/cm^2 is applied at the base of microchannels projected area (L_{ch}× W_{HS}). To save the simulation time, only half part of heat sink is considered for the numerical analysis by adopting the symmetry boundary condition at the center plane. All other outside walls are assumed to be adiabatic. For solution of the governing equations (Eqs. (2)-(5)) commercial CFD software, ANSYS Fluent 14.0 is used. SIMPLE algorithm [57] is used for the pressure-velocity coupling and second order upwind scheme is selected for the spatial

discretization of momentum and energy equations. The standard discretization technique is used for obtaining pressure value.

C. Data Reduction

1. Calculation of Flow Maldistribution Factor

To estimate extend of flow distribution non-uniformity, flow maldistribution factor (ϕ) is calculated at each row of primary channels. For that purpose mass flow rate across each primary channel is calculated at the center of associated neighboring fins. Flow maldistribution factor for MPFHS is calculated as given below:

$$\phi = \frac{\sum_{N=1}^{20} \left| \frac{\dot{m}_{\max} - \dot{m}_{\min}}{\dot{m}_{\text{avg}}} \right|_N}{20} \tag{6}$$

Where, N (N = 1, 2, 3…20) represents pin fin rows along the flow length.

2. Nusselt Number

The Nusselt number is defined as:

$$Nu = \frac{hD_{\text{h}}}{k_{\text{f}}} \tag{7}$$

And the heat transfer coefficient (h):

$$h = \frac{q_{\Gamma}''}{(T_{\Gamma,\text{avg}} - T_{\text{f,vavg}})} \tag{8}$$

q_{Γ}'' and $T_{\Gamma,\text{avg}}$ are the heat flux supplied and surface temperature at solid-fluid interface of pin finned region. $T_{f,vavg}$ is volumetric average temperature of fluid. $T_{\Gamma,\text{avg}}$ and $T_{\text{f,vavg}}$ are calculated as:

$$T_{\Gamma,\text{avg}} = \iint \frac{T_{\Gamma} d\Gamma}{\Gamma} \tag{9}$$

$$T_{\text{f,vavg}} = \iiint \frac{T dV_{\text{f}}}{dV_{\text{f}}} \tag{10}$$

3. Thermal-hydraulic performance index (η)

The thermal-hydraulic performance index is calculated as:

$$\eta = \left(\frac{\mathrm{Nu_{PD-MPFHS}}}{\mathrm{Nu_{CD-MPFHS}}}\right) / \left(\frac{\Delta P_{\mathrm{PD-MPFHS}}}{\Delta P_{\mathrm{CD-MPFHS}}}\right)^{1/3} \quad (11)$$

III. Grid Independence and Validation

Grid independence test is carried out at highest $\mathrm{Re_{in}}$ to insure the accuracy of current numerical results. Three different grid schemes: course grid, fine grid and very fine grid schemes are adopted. Results of maximum temperature and overall pressure drop are compared for CD-MPFHS as given in Table 3. It is noticed that absolute percentage deviation (ε) between fine and very fine grid schemes is less than 1% for both parameters. Similar grid independence procedure is performed for PD-MPFHS and ε is noticed to be less than 1% between fine and very fine grid schemes.

Results of CD-MPFHS are validated for the Nusselt number with Liu et al. [58] and for the friction factor with correlation of Cao et al. [59] as shown in Figs. 2(a) and 2(b) respectively. These correlations are given by Eqs. (12) and (13) respectively. It is noticed that application range of Reynolds number of both correlation lies within the boundary conditions of present study. Mean absolute deviation of 3.2% and 10% are observed in prediction of the Nusselt number and the friction factor respectively.

$$Nu_{\mathrm{fin}} = 0.1245\, Re_{\mathrm{fin}}^{0.6106} Pr_{\mathrm{f,avg}}^{0.36} \left(\frac{Pr_{\mathrm{f,avg}}}{Pr_{\mathrm{s,avg}}}\right)^{0.25} \quad (12)$$

$$f = 76.02\, Re_{\mathrm{avg}}^{-0.94} \quad (13)$$

Where, Re_{fin} and $Re_{\mathrm{avg}}$are Reynolds number based on fin hydraulic diameter and Reynolds number based average velocity through channel as described in [58] and [59] respectively.

IV. Results and Discussion

A. Flow Distribution Analysis

Fluid flow inside the MPFHS can be classified in two types: Primary flow – the flow occurring between micro pin fins (inside channels) in the longitudinal flow direction and Secondary flow- the flow occurring between micro pin fins in the transverse to the primary flow direction [45].

1. *Flow Distribution in Primary Channels*

Figures 3(a) and 3(b) show the fluid flow distribution pattern in the primary channels of the CD-MPFHS and PD-MPFHS respectively. As reported by [54] that the formation of recirculation zones due to the sudden expansion of fluid inside inlet manifold is responsible for the uneven distribution of fluid across channels. In comparison to the CD-MCHS (ϕ = 0.79), the flow non-uniformity problem is found more severe for the CD-MPFHS (ϕ = 0.94). The basic reason for the increase in maldistribution of CD-MPFHS is increase in mass flow rate of fluid flowing through central channels of CD-MPFHS due to the presence of the secondary channels. Analogous to the PD-MCHS, increase in width of the central micro pin fins for the PD-MPFHS (decrease in size of central channels) helps in reducing the fluid flow through the central channels. Similarly, the reduction in the width of side micro pin fins (increase in size of the side channels) increases the fluid amount flowing through them. The average non-uniformity of flow across primary channels (ϕ) reduces to 0.6 for the PD-MPFHS. Figure 4 shows the velocity contour plots for the CD-MPFHS and PD-MPFHS, it can be noticed that velocity non-uniformity across and along the channels is less harsh for the PD-MPFHS.

2. *Flow Distribution in Secondary Channels*

The fluid flow in the secondary channels is equally important. It ensures the frequent mixing of the fluid flowing in the primary channels. Frequent mixing of the fluid normalizes the fluid temperature across heat sink, which ultimately helps in maintaining the uniform surface temperature of the heat sink. Figure 5 shows the fluid flow distribution of the secondary channels for the CD-MPFHS and PD-MPFHS. Four types of secondary and primary flow interactions have been observed as shown in Figs. 6(a)-6(d). Where, $\dot{m}_{x1}$ and $\dot{m}_{x2}$ represent secondary flow entering and leaving a secondary channel, respectively. Similarly, $\dot{m}_{y1}$ and $\dot{m}_{y2}$ represent flow entering and leaving a primary channel respectively. In Case 1 (Fig. 6(a)) – the fluid in the secondary channels have tendency to flow from the central channels towards side channels. Whereas in Case 2 (Fig. 6(b)) – the fluid flow behavior in the secondary channels reverses and the fluid starts flowing from the side channels towards central channels. As evident from the Figs. 3(a) and 3(b) that in general the flow in the primary channels of the central micro pin fins (for both designs) decreases initially then attains minima and subsequently starts increasing towards the exit end. However, for the side micro pin fins – flow in the primary channel in general increase attains maxima then starts decreasing towards the exit end. The dominance of Case 1 and Case 2 in the upstream and downstream half of flow field is

primarily responsible for the observed behavior. Thus, direction of flow field in the neighboring secondary channels also regulates the flow pattern of the primary channels in MPFHS. Case 3 (Fig. 6(c)) has been observed on the interacting locations of Case 1 and Case 2. Similarly, Case 4 (Fig. 6(d)) has been observed in the central channel only. It is evident from the Fig. 5 that the secondary flow is higher in the PD-MPFHS in comparison to CD-MPFHS.

B. Thermal Performance

1. *Temperature Distribution*

It is found by numerical results of the CD-MCHS and CD-MPFHS designs that micro pin fin arrangement offer significant reduction in maximum temperature ($T_{b,max}$ reduces by 6.0 K) and average temperature ($T_{b,avg}$ reduces by 7.2 K) in comparison to the CD-MCHS at design conditions (Re_{in}=1200). Intermixing of fluid flowing in the primary channels (through secondary flow passages) and the redevelopment of thermal boundary layer due to flow interruption are concurrently responsible for the above observation. Figure 7 compares the temperature contours of the CD-MPFHS and the PD-MPFHS designs. It is evident that in comparison to CD-MPFHS – base surface temperature non-uniformity problem is less severe for the PD-MPFHS. As CD-MPFHS suffers from high unevenness of flow distribution with maximum cooling fluid flowing through the central channels and very less fluid flows through the side channels. As a result, more heating of side channels occurs. PD-MPFHS on the other hand offers better flow distribution across primary channels, permitting less flow through central primary channels and more flow through side primary channels. Also, the secondary fluid flow in the PD-MPFHS is stronger than CD-MPFHS promoting rigorous mixing of fluid flowing in primary channels. The total secondary flow for PD-MPFHS is almost 36% higher than CD-MPFHS. Under the combined influence of normalized primary flow distribution and the stronger secondary flow, maximum and average temperatures are reduced by 4.6 K and 2.2 K for PD-MPFHS as compared to CD-MPFHS at design conditions. Base surface temperature non-uniformity ($T_{b,max}$ - $T_{b,min}$) also eases from 47 K to 42.5 K by the PD-MPFHS. Figure 8 compares maximum base temperature ($T_{b,max}$), average base temperature ($T_{b,avg}$) and base temperature fluctuation ($T_{b,max}$ - $T_{b,min}$) of CD-MPFHS and PD-MPFHS at different flow rates. It is noticed that PD-MPFHS provides more effective cooling and uniform base temperature even at off-design conditions at different Re_{in}. However, further decreasing Re_{in} to 500 results in the reduction of $T_{b,avg}$ benefit up to 0.7 K only, but maximum temperature improvement remains consistent (~5 K) for the PD-MPFHS, which proves the potential of proposed design for the mitigation of hot spot problem. Furthermore, it is

observed that the perks of PD-MPFHS escalate with an increase of heat flux and at the applied heat flux of 150 W/cm^2; the maximum and average temperature reduces up to 6.2 K and 3.0 K, respectively for the PD-MPFHS as compared to CD-MPFHS.

2. Heat Transfer Analysis

Heat transfer performance of the CD-MPFHS and the PD-MPFHS are compared by their Nusselt number values. Figure 9 shows the comparison of Nusselt number for the CD-MPFHS and the PD-MPFHS at different Reynolds numbers. It is noticed that PD-MPFHS offers 10.1% improvement in the Nusselt number at the reference design condition. Although, its total heat transfer area is around 2.3% lower than CD-MPFHS. Improved hydrodynamics of flowing fluid (uniform distribution of fluid in the primary channels and the enriched secondary fluid flow) is responsible for heat transfer intensification provided by the PD-MPFHS. However, it is found that pressure drop across PD-MPFHS is 5.7% higher than CD-MPFHS at design conditions. High fluid flow resistance offered by the central channels (narrow for PD-MPFHS) of the PD-MPFHS is responsible for the observed behavior. Figure 10 compares the overall pressure drop of MPFHSs at different Re_{in}.

Therefore, to identify the usefulness of the proposed design, thermal-hydraulic performance index is calculated by using Eq. (11) at different Re_{in} as given in Table 4. It is noticed that average thermal-hydraulic performance index for the PD-MPFHS is 7.5% higher for the studied range of Re_{in}, which indicates its superior heat transfer characteristics

V. Conclusions

In current numerical study, the effect of flow normalization in micro pin finned heat sink has been carried out. Two types of MPFHS: one with uniform width of pin fins (CD-MPFHS) and another with variable width of pin fins (PD-MPFHS) are generated following the previous study [54] of the current authors. Three-dimensional numerical analysis of both geometries is carried out to study the effect of flow maldistribution on pin finned heat sinks. Following are the main findings of the current study:

1) Both MPFHSs showed higher liquid flow non-uniformity in comparison to their respective parent MCHS design.

2) Better liquid flow distribution is noticed for PD-MPFHS as compared to CD-MPFHS. Non-uniformity of mass flow rate (maldistribution) reduces 36% for PD-MPHS as compared to CD-MPFHS in primary channels. Uniformity of mass flow rate in the primary channels also facilitated in boosting the liquid flow rate through the secondary channels. Secondary channels fluid flow ensures frequent mixing of fluid flowing in primary channels. Total fluid flow rate across the secondary channels is around 36% higher for the PD-MPFHS.
3) Due to the better flow distribution of fluid among primary channels and the higher fluid flow across secondary channels in PD-MPFHS – maximum and average base temperatures are reduced by 4.6 K and 2.2 K as compared to CD-MPFHS.
4) Nusselt number increases by 10.1% for the PD-MPFHS. However, PD-MPFHS suffer from the pressure drop penalty of 5.7 % in comparison to CD-MPFHS. PD-MPFHS gives better thermal-hydraulic performance index for the entire studied Reynolds number range.

Acknowledgment

The authors acknowledge financial help provided by the Department of Science and Technology, India, and Ministry of Science and Higher Education, Poland (DST/INT/Pol/P-29/2016) for carrying our current work. The funding organizations had not played any role in study design, decision to publish or preparation of the manuscript.

References

[1] Almoli, A. Thompson, A., Kapur, N., Summers, J., Thompson, H., and Hannah, G., "Computational Fluid Dynamic Investigation of Liquid Rack Cooling in Data Centres,'' *Applied Energy*, Vol. 89, No. 1, 2012, pp. 150-155. DOI:10.1016/j.apenergy.2011.02.003.

[2] Ellsworth, M. J., Goth, G. F., Zoodsma, R. J., Arvelo, A., Campbell, L. A., and Anderl, W. J., "An Overview of the IBM Power 775 Supercomputer Water Cooling System,'' *Journal of Electronic Packaging*, Vol. 134, No. 2, 2012, p. 020906. DOI: 10.1115/1.4006140.

[3] Kandlikar, S. G., "Review and Projections of Integrated Cooling Systems for Three-Dimensional Integrated Circuits,'' *Journal of Electronic Packaging, Vol.* 136, No. 2, 2014, Paper 024001. DOI: 10.1115/1.4027175.

[4] Tuckerman, D. B., and Pease, R. F. W., "High-Performance Heat Sinking for VLSI,'' *IEEE Electron Device Letters*, Vol. 2, No. 5, 1981, pp. 126-129. DOI: 10.1109/EDL.1981.25367.

[5] Cheng, L., Thome, J. R., "Cooling of Microprocessors Using Flow Boiling of CO_2 in a Micro-Evaporator: Preliminary Analysis and Performance Comparison,'' *Applied Thermal Engineering*, Vol. 29, No. 11-12, 2009, pp. 2426–2432. DOI:10.1016/j.applthermaleng.2008.12.019.

[6] Lee, J., and Mudawar, I, "Two-Phase Flow in High-Heat-Flux Micro-Channel Heat Sink for Refrigeration Cooling Applications: Part I-Pressure Drop Characteristics,'' *International Journal of Heat and Mass Transfer*, Vol. 48, No. 5, pp. 928-940. DOI:10.1016/j.ijheatmasstransfer.2004.09.018.

[7] El-Masri, M. A., and Louis, J. F., "On the Design of High-Temperature Gas Turbine Blade Water Cooling Channels,'' *Journal of Engineering for Power*, Vol. 100, No. 4, 1978, pp. 586–591. https://doi.org/10.1115/1.3446400.

[8] Nacke, R., Northcutt, B., and Mudawar,, "Theory and Experimental Validation of Cross-Flow Micro-channel Heat Exchanger Module with Reference to High Mach Aircraft Gas Turbine Engines,'' *International Journal of Heat and Mass Transfer*, Vol. 54, No. 5-6, 2011, pp. 1224-1235. DOI:10.1016/j.ijheatmasstransfer.2010.10.028.

[9] Missaggia, I. J, Walpole, J. N., Liau, Z. L., and Phillips, R. J., "Microchannel Heat Sinks for Two-Dimensional High-Power-Density Diode Laser Arrays,'' *IEEE Journal of Quantum Electronics*, Vol. 25, No. 9, 1989, pp. 1988-1992. DOI: 10.1109/3.35223.

[10] Tripathi, S., Prabhakar, A., Kumar, N., Singh, S.G., and Agrawal, A., "Blood Plasma Separation in Elevated Dimension T-Shaped Microchannel,'' *Biomed Microdevices*, Vol. 15, No. 3, 2013, pp. 415-425. DOI: 10.1007/s10544-013-9738-z.

[11] Kanno, K., Kawazumi, H., Miyazaki, M., Maeda, H., and Fujii, M., "Enhanced Enzymatic Reactions in a Microchannel Reactor,'' *Australian Journal of Chemistry*, Vol. 55, No. 11, 2002, pp. 687-690. DOI: 10.1071/CH02171.

[12] Abiev, R.Sh., Pavlyukova,Y. N., Nesterova, O. M., Svetlov, S. D., and Ostrovskii, V. A., "Mass Transfer Intensification of 2-Methyl-5-Nitrotetrazole Synthesis in Two-Phase Liquid–Liquid Taylor Flow in Microreactor,'' *Chemical Engineering Research and Design*, Vol. 144, 2019, pp. 444-458. https://doi.org/10.1016/j.cherd.2019.01.033.

[13] Qu, W., and Mudawar, I., "Experimental and Numerical Study of Pressure Drop and Heat Transfer in a Single-Phase Micro-channel Heat Sink,'' *International Journal of Heat and Mass Transfer*, Vol. 45, No. 12, 2002, pp. 2549-2565. https://doi.org/10.1016/S0017-9310(01)00337-4.

[14] Liu, D., and Garimella, S. V., "Investigation of Liquid Flow in Microchannels,'' *Journal of Thermophysics and Heat Transfer*, Vol. 18, No. 1, 2004, pp. 65-72. 2004. https://doi.org/10.2514/1.9124.

[15] Steinke, M. E., and Kandlikar, S. G., "Single-Phase Liquid Friction Factors in Microchannels,'' *International Journal of Thermal Science*, Vol. 45, No. 11, 2006, pp. 1073-1083. DOI:10.1016/j.ijthermalsci.2006.01.016.

[16] Rosa, P., Karayiannis, T., and Collins, M., "Single-Phase Heat Transfer in Microchannels: The Important of Scaling Effects,'' *Applied Thermal Engineering*, Vol. 29, No. 17-18, 2009, pp. 3447–3468. https://doi.org/10.1016/j.applthermaleng.2009.05.015

[17] Huang, C.-Y, Wu, C.-M., Chen, Y.-N., and Liou, T.-M., "The Experimental Investigation of Axial Heat Conduction Effect on the Heat Transfer Analysis in Microchannel Flow,'' *International Journal of Heat and Mass Transfer*, Vol. 70, 2014, pp. 169–173. https://doi.org/10.1016/j.ijheatmasstransfer.2013.10.059.

[18] Sahar, A., Ozdemir, M. R., Fayyadh, E. M., Wissink, J., Mahmoud, M. M., and Karayiannis, T. G., "Single Phase Flow Pressure Drop and Heat Transfer in Rectangular Metallic Microchannels," *Applied Thermal Engineering*, Vol. 93, 2016, pp. 1324–1336. doi:10.1016/j.applthermaleng.2015.08.087.

[19] Kadam, S.T., Kumar, R., and Abiev, R., "Performance Augmentation of Single-Phase Heat Transfer in Open-Type Microchannel Heat Sink," *Journal of Thermophysics and Heat Transfer*, Vol. 33, No. 2, 2019, pp. 416-424. https://doi.org/10.2514/1.T5522.

[20] Go, J. S., "Design of a Microfin Array Heat Sink Using Flow-Induced Vibration to Enhance the Heat Transfer in the Laminar Flow Regime," *Sensors and Actuators A: Physical*, Vol. 105, No. 2, 2003, pp. 201–210. https://doi.org/10.1016/S0924-4247(03)00101-8

[21] Chandratilleke, T. T., Jagannatha, D., and Narayanaswamy, R., "Heat Transfer Enhancement in Microchannels with Cross-Flow Synthetic Jets," *International Journal of Thermal Science*, Vol. 49, No. 3, 2010, pp. 504–513. DOI:10.1016/j.ijthermalsci.2009.09.004.

[22] Wang, Y., and Peles, Y., "An Experimental Study of Passive and Active Heat Transfer Enhancement in Microchannels," *Journal of Heat Transfer*, Vol. 136, No. 3, 2013, Paper 031901. DOI: 10.1115/1.4025558.

[23] Yadav, V., Baghel, K., Kumar, R., and Kadam, S. T., "Numerical Investigation of Heat Transfer in Extended Surface Microchannels," *International Journal of Heat and Mass Transfer*, Vol. 93, 2016, pp. 612-622. https://doi.org/10.1016/j.ijheatmasstransfer.2015.10.023.

[24] Klugmann, M., Dabrowski, P., and Mikielewicz, D., "Pressure Drop Related to Flow Maldistribution in a Model Minichannel Plate Heat Exchanger," *Archives of Thermodynamics*, Vol. 39, No. 2, 2018, pp. 123-146. DOI: 10.1515/aoter-2018-0015.

[25] Li, X. Y., Wang, S. L., Wang, X. D., and Wang, T. H., "Selected Porous-Ribs Design for Performance Improvement in Double-Layered Microchannel Heat Sinks," *International Journal of Thermal Science*, Vol. 137, 2019, pp. 616-626. https://doi.org/10.1016/j.ijthermalsci.2018.12.029.

[26] Khan, A. A., Kim, S.-M., and Kim, K.-Y. "Performance Analysis of a Microchannel Heat Sink with Various Rib Configurations," *Journal of Thermophysics and Heat Transfer*, Vol. 30, No. 4, 2016, pp. 782-790. https://doi.org/10.2514/1.T4663.

[27] Xia, G., Zhai, Y., and Chi, Z., "Numerical Investigation of Thermal Enhancement in a Micro Heat Sink with Fan-Shaped Reentrant Cavities and Internal Ribs," *Applied Thermal Engineering*, Vol. 58, No. 1-2, 2013, pp. 52-60. https://doi.org/10.1016/j.applthermaleng.2013.04.005.

[28] Sui, Y., Teo, C. J., Lee, P. S., Chew, Y. T., and Shu, C., "Fluid Flow and Heat Transfer in Wavy Microchannels," *International Journal of Heat and Mass Transfer*, Vol. 53, No. 13-14, 2010, pp. 2760-2772. DOI:10.1016/j.ijheatmasstransfer.2010.02.022.

[29] Chai, L., and Wang, L. "Thermal-Hydraulic Performance of Interrupted Microchannel Heat Sinks with Different Rib Geometries in Transverse Microchambers," *International Journal of Thermal Science*, Vol. 127, 2018, pp. 201-212. https://doi.org/10.1016/j.ijthermalsci.2018.01.029.

[30] Lu, G., and Zhai, X., "Analysis on Heat Transfer and Pressure Drop of a Microchannel Heat Sink with Dimples and Vortex Generators," *International Journal of Thermal Science*, Vol. 145, 2019, Paper 105986. https://doi.org/10.1016/j.ijthermalsci.2019.105986.

[31] Malvandi, A., Moshizi, S. A., and Ganji, D. D., "Nanofluids Flow in Microchannels in Presence of Heat Source/Sink and Asymmetric Heating," *Journal of Thermophysics and Heat Transfer*, Vol. 30, No. 1, 2016, pp. 111-119. https://doi.org/10.2514/1.T4562.

[32] Li, Y., Yao, S.-C., "Porous Media Modeling of Microchannel Cooled Electronic Chips with Nonuniform Heating," *Journal of Thermophysics and Heat Transfer*, Vol. 29, No. 4, 2015, pp. 695-704. https://doi.org/10.2514/1.T4509.

[33] Chauhan, A., Sammakia, B., Ghose, K., Refai-Ahmed, G., and Agonafer, D., "Hot Spot Mitigation Using Single-Phase Microchannel Cooler for Microprocessors," *Proceedings 12th IEEE Intersociety Conference on Thermal*

Thermomechanical Phenomena in Electronic Systems, 2-5 June 2010, pp. 1-11. DOI**:** 10.1109/ITHERM.2010.5501357.

[34] Kishimoto, T., and Saski, S., "Cooling Characteristics of Diamond-Shaped Interrupted Cooling Fin for High-Power LSI Devices," *Electronic Letters*, Vol. 23, No. 9, 1985, pp. 456–457. DOI: 10.1049/el:19870328.

[35] Steinke, M. E., and Kandlikar, S. G., "Review of Single-Phase Heat Transfer Enhancement Techniques for Application in Microchannels, Minichannels and Microdevices," *International Journal of Heat Technology*, Vol. 22, No. 2, 2004, pp. 3–11. DOI: 10.18280/ijht220201.

[36] Kosar, A., Mishra, C., and Peles, Y. "Laminar Flow Across a Bank of Low Aspect Ratio Micro Pin Fins," *Journal of Fluids Engineering*, Vol. 127, No. 3, 2005, pp. 419-430. DOI: 10.1115/1.1900139.

[37] Peles, Y., Kosar, A., Mishra, C., and Kuo, C. J., and Schneider, B., "Forced Convective Heat Transfer across a Pin Fin Micro Heat Sink," *International Journal of Heat and Mass Transfer*, Vol. 48, No. 17, 2005, pp. 3615-3627. DOI:10.1016/j.ijheatmasstransfer.2005.03.017.

[38] Kosar, A., and Peles, Y., "Convective Flow of Refrigerant R-123 Across a Bank of Micro Pin Fins," *International Journal of Heat and Mass Transfer*, Vol. 49, No. 17-18, 2006, pp. 3142-3155. DOI:10.1016/j.ijheatmasstransfer.2006.02.013.

[39] Kosar, A., and Peles, Y., "Micro Scale Pin Fin Heat Sinks—Parametric Performance Evaluation Study," *IEEE Transactions on Components and Packaging Technologies*, Vol. 30, No. 4, 2007, pp. 855–865. DOI: 10.1109/TCAPT.2007.906334.

[40] Qu, W., and Siu-Ho, A., "Liquid Single-Phase Flow in an Array of Micro Pin Fins—Part 1: Heat Transfer Characteristics," *Journal of Heat Transfer*, Vol. 130, No. 12, 2008, p. 122402. DOI: 10.1115/1.2970080.

[41] Lee, Y. J., Lee, P. S., and Chou, S. K., "Enhanced Microchannel Heat Sinks Using Oblique Fins," in Proc. 2009 ASME InterPACK Conference, San Francisco, California, USA, 19-23 July, 2009 Paper No. IPACK2009-89059. https://doi.org/10.1115/InterPACK2009-89059.

[42] John, T.J., Mathew, B., and Hegab, H., "Parametric Study on the Combined Thermal and Hydraulic Performance of Single-Phase Micro Pin-fin Heat Sinks Part I: Square and Circle Geometries," *International Journal of Thermal Science*, Vol. 49, No. 11, 2010, pp. 2177-2190. DOI:10.1016/j.ijthermalsci.2010.06.011.

[43] Hasan, M. I., "Investigation of Flow and Heat Transfer Characteristics in Micro Pin Fin Heat Sink with Nanofluid," *Applied Thermal Engineering*, Vol. 63, No. 2, 2014, pp. 598-607. DOI: 10.1016/j.applthermaleng.2013.11.059.

[44] Duangthongsuk, W., and Wongwises, S., "A Comparison of the Heat Transfer Performance and Pressure Drop of Nanofluid-Cooled Heat Sinks with Different Miniature Pin Fin Configuration," *Experimental Thermal Fluid Science*, Vol. 69, 2015, pp. 111–118. http://dx.doi.org/10.1016/j.expthermflusci.2015.07.019.

[45] Mou, N., Lee, Y. J., Lee, P. S., Singh, P. K., and Khan, S. A., "Investigations on the Influence of Flow Migration on Flow and Heat Transfer in Oblique Fin Microchannel Array," *Journal of Heat Transfer*, Vol. 138, No. 10, 2016, Paper 102403. DOI: 10.1115/1.4033540.

[46] Mohammadi, A., and Kosar, A., "Hydrodynamic and Thermal Performance of Microchannels with Different In-Line Arrangements of Cylindrical Micro Pin Fins," *Journal of Heat Transfer*, Vol. 138, No. 12, 2016, Paper 122403. DOI: 10.1115/1.4034164.

[47] Mohammadi, A., and Kosar, A., "Hydrodynamic and Thermal Performance of Microchannels with Different Staggered Arrangements of Cylindrical Micro Pin Fins," *Journal of Heat Transfer*, Vol. 139, No. 6, 2017, Paper 062402. DOI: 10.1115/1.4035655.

[48] Xu, F. and Wu, H., "Experimental Study of Water Flow and Heat Transfer in Silicon Micro-Pin-Fin Heat Sinks," *Journal of Heat Transfer*, Vol. 140, No. 12, 2018, Paper 122401. DOI: 10.1115/1.4040956.

[49] Lu, M. C., and Wang, C. C., "Effect of Inlet Location on the Performance of Parallel-Channel Cold Plate," *IEEE Transactions on Components and Packaging Technologies*, Vol. 29, No. 1, 2006, pp. 30-38. DOI**:** 10.1109/TCAPT.2005.850539.

[50] Chein, R., and Chen, J., "Numerical Study of the Inlet/Outlet Arrangement Effect on Microchannel Heat Sink Performance," *International Journal of Thermal Science*, Vol. 48, No. 8, 2009, pp. 1627-1638. DOI:10.1016/j.ijthermalsci.2008.12.019.

[51] Siva, V. M., Pattamatta, A., and Das, S. K., "Investigation on Flow Maldistribution in Parallel Microchannel Systems for Integrated Microelectronic Device Cooling," *IEEE Transactions on Components and Packaging Technologies*, Vol. 4, No. 3, 2014, pp. 438-450. DOI: 10.1109/TCPMT.2013.2284291.

[52] Xia, G. D., Jiang, J., Wang, J., Zhai, Y. L., and Ma, D. D., "Effects of Different Geometric Structures on Fluid Flow and Heat Transfer Performance in Microchannel Heat Sinks," *International Journal of Heat and Mass Transfer*, Vol. 80, 2015, pp. 439-447. https://doi.org/10.1016/j.ijheatmasstransfer.2014.08.095.

[53] Dabrowski, P., Klugmann, M., and Mikielewicz, D., "Selected Studies of Flow Maldistribution in a Minichannel Plate Heat Exchanger," *Archives of Thermodynamics*, Vol. 38, No. 3, 2017, pp. 135-148. DOI: 10.1515/aoter-2017-0020.

[54] Kumar, R., Singh, G., and Mikielewicz, D., "A New Approach for the Mitigating of Flow Maldistribution in Parallel Microchannel Heat Sink," *Journal of Heat Transfer*, Vol. 140, No. 7, 2018, Paper 072401. DOI: 10.1115/1.4038830.

[55] Yadav, V., Kumar, R., and Narain, A., "Mitigation of Flow Maldistribution in Parallel Microchannel Heat Sink," *IEEE Transactions on Components, Packaging and Manufacturing Technology*, Vol. 9, No. 2, 2018, pp. 247-261. DOI: 10.1109/TCPMT.2018.2851543.

[56] Kumar, R., Singh, G., and Mikielewicz, D., "Numerical Study on Mitigation of Flow Maldistribution in Parallel Microchannel Heat Sink: Channels Variable Width versus Variable Height Approach," *Journal of Electronic Packaging*, Vol. 141, No. 2, 2019, Paper 021009. DOI: 10.1115/1.4043158.

[57] Patankar, S. V., "*Numerical Heat Transfer and Fluid Flow*," Hemisphere, Washington, DC, 1980.

[58] Liu, M., Liu, D., Xu, S., Chen, Y., "Experimental study on liquid flow and heat transfer in micro square pin fin heat sink," *International Journal of Heat and Mass Transfer*, Vol. 54, No. 25-26, 2011, pp. 5602–5611. DOI:10.1016/j.ijheatmasstransfer.2011.07.013.

[59] Cao, H. S., Vanapalli, S., Holland, H. J., Vermeer, C. H., Brake, H. J. M. ter, "Heat Transfer and Pressure Drop in Microchannels with Isotropically Etched Pillars at Sub-ambient Temperatures," *International Journal of Refrigeration*, Vol. 98, 2019, pp-334-342. https://doi.org/10.1016/j.ijrefrig.2018.10.005.

Table Captions List

Figure Captions List

Table 1 Dimension of MCHS and MPFHS designs

Parameter	L_{HS}	L_{ch}	L_M	W_{HS}	W_M	H_{HS}	H_{ch}
Value (mm)	18	10	3.6	13.54	12.74	0.5	0.4

Table 2 Primary channel width and fin width (μm) for PD-MPFHS

i/*e*	1	2	3	4	5	6	7	8	9	10	11	12	13
$W_{ch,i}$	332	343	346	347	343	333	302	261	234	216	205	200	199
$W_{fin,e}$	146	176	175	176.5	182.5	201	237.5	272.5	294.5	308.5	317	320.5	-

Note: Dimension of other half of channels (*i*=14-25) and fins (*e*=13-24) are assumed symmetric to reported channels (*i*=12-1) and fins (*e*=12-1) respectively.

Table 3 Results of Grid independence analysis

Grid schemes	No. of elements	T_{max} (K)	ε	ΔP (Pa)	ε
Coarse grids	6182795	336.7	0.18	12868.3	3.64
Fine grids	19320680	337.3	0.03	13355.0	0.41
Very fine grids	37162786	337.2		13300.8	

Table 4 Thermal-hydraulic performance index (η) for different Re_{in}

Re_{in}	800	1000	1200	1400	1600
η	1.06	1.07	1.08	1.09	1.08

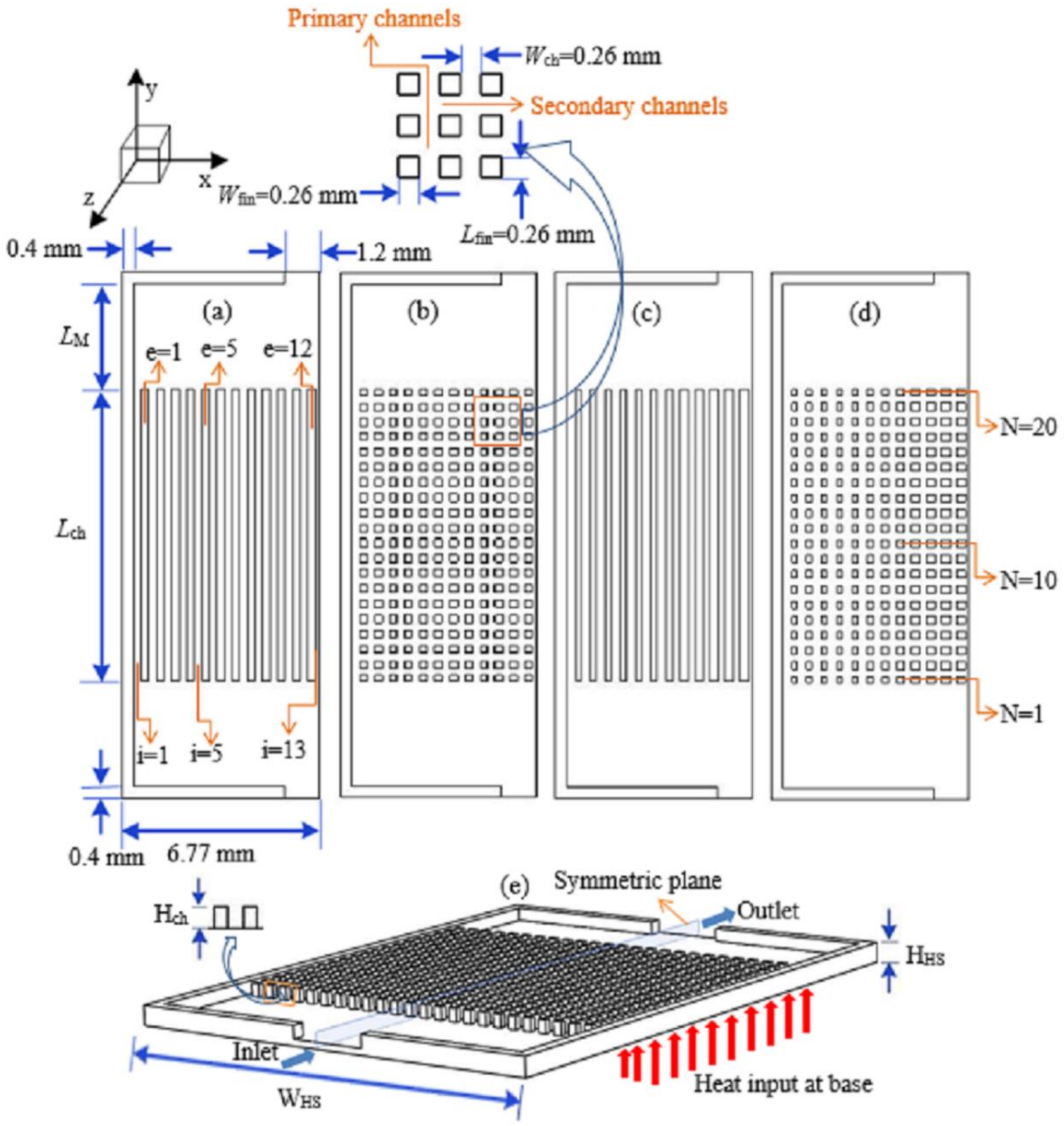

Fig. 1 Geometric configuration of different designs (a) CD-MCHS, (b) CD-MPFHS, (C) PD-MCHS, (d) PD-MPFHS, and (e) 3D view of full CD-MPFHS

115×122 mm (300×300 DPI)

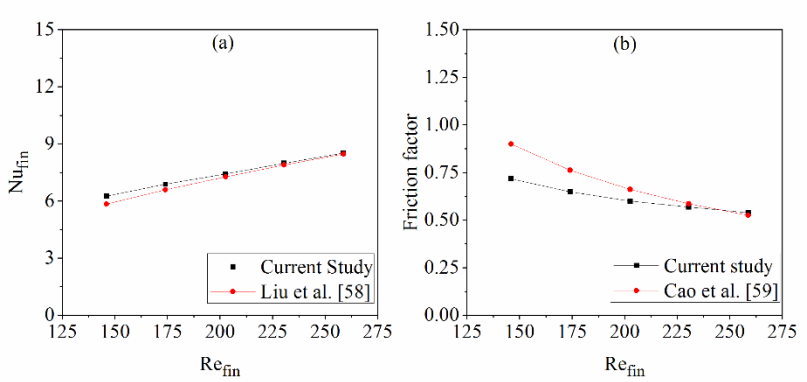

Fig. 2 Comparison of numerical results with correlations (a) Nusselt number and (b) friction factor for CD-MPFHS

206×98mm (300×300 DPI)

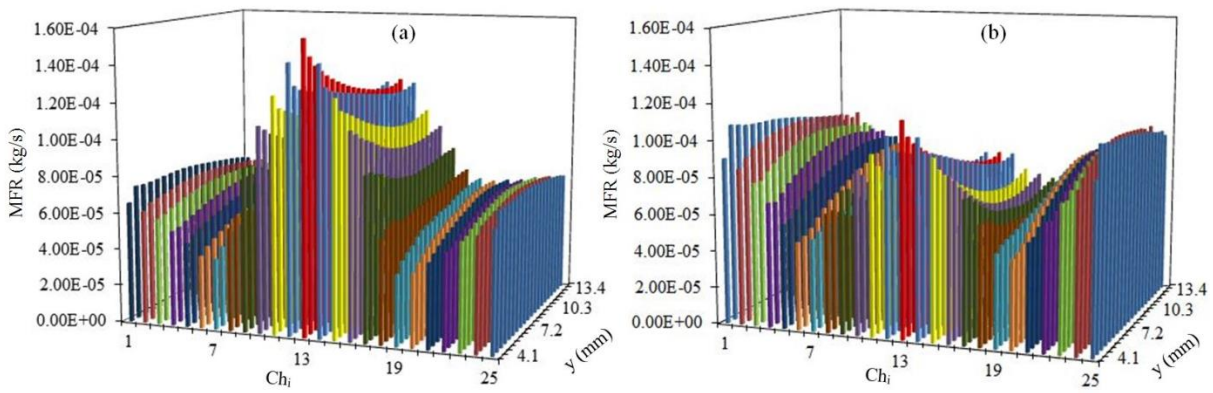

Fig. 3 Mass flow rate distribution in primary channels of (a) CD-MPFHS and (b) PD-MPFHS at different locations along the flow direction

140×46mm (300×300 DPI)

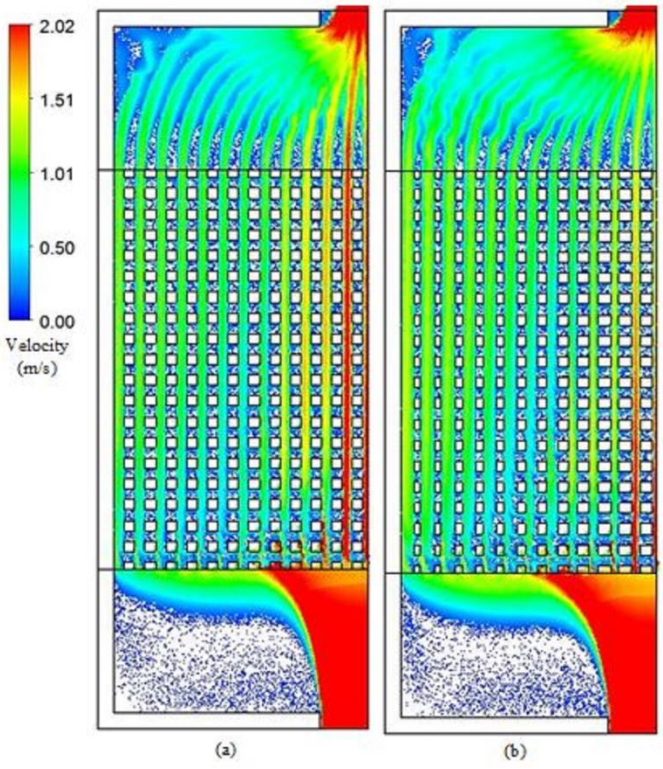

Fig. 4 Velocity contour at the center plane of (a) CD-MPFHS and (b) PD-MPFHS

70×80mm (300×300 DPI)

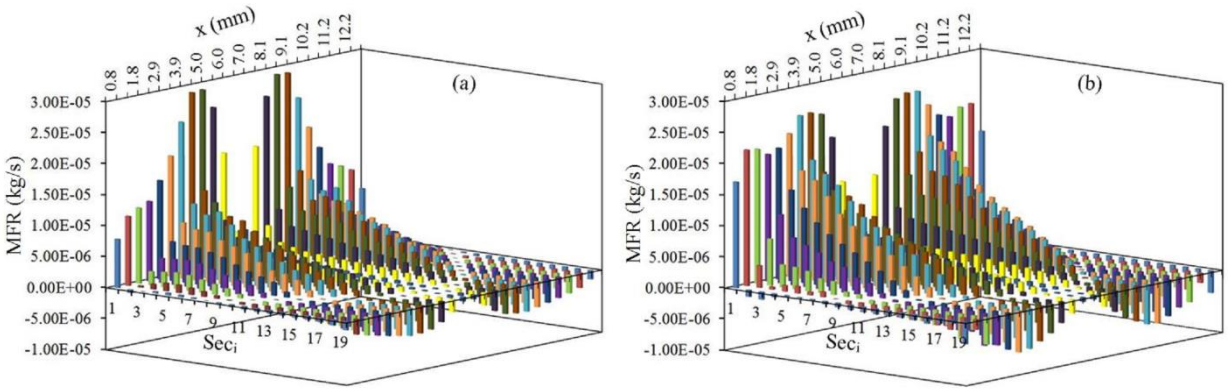

Fig. 5 Mass flow rate distribution in secondary channels (a) CD-MPFHS and (b) PD-MPFHS for all rows along the flow length

192×63mm (300×300 DPI)

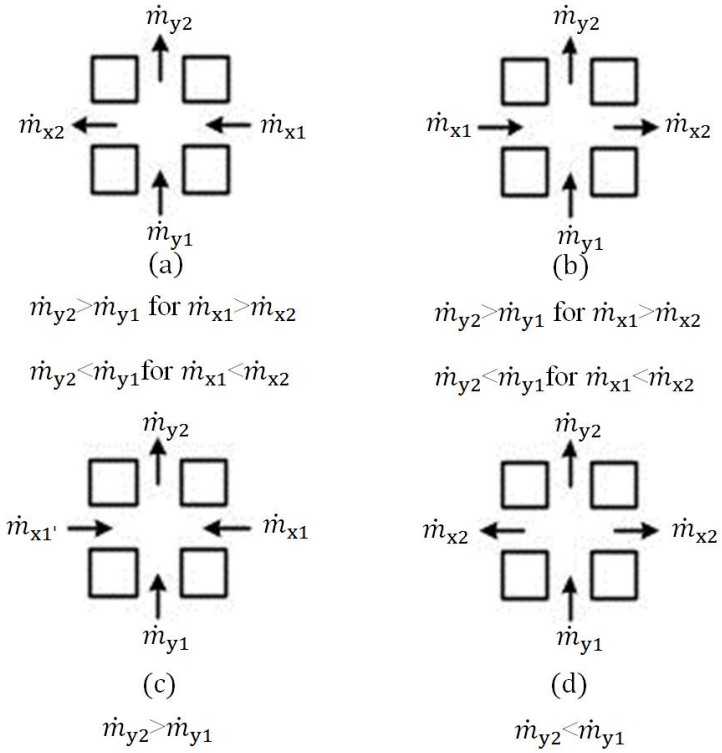

Fig. 6 Types of primary and secondary flow interactions in MPFHSs (a) Case 1, (b) Case 2, (c) Case 3 and

(d) Case 4

74×77mm (300×300 DPI)

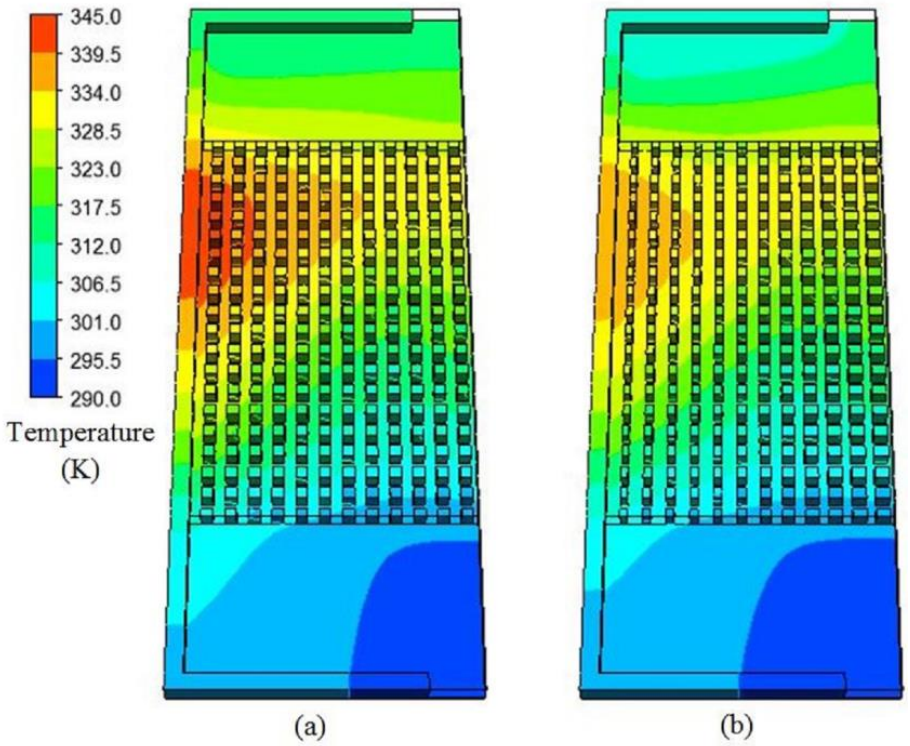

Fig. 7 Temperature contours for (a) CD-MPFHS and (b) PD-MPFHS

96×82mm (300×300 DPI)

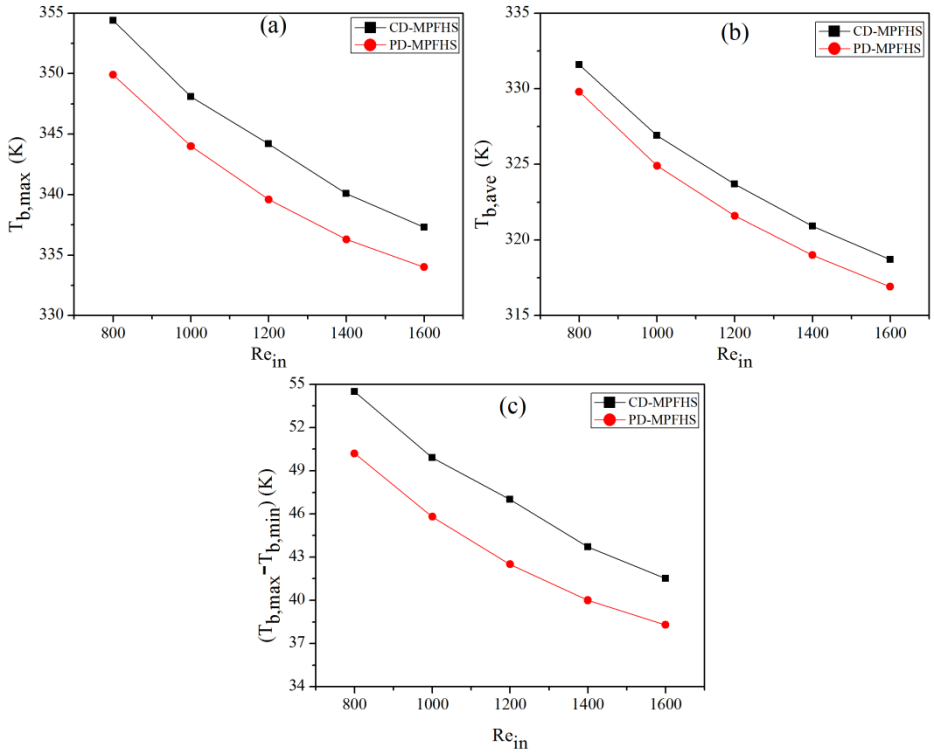

Fig. 8 Effect of Reynolds number (Re_{in}) on (a) maximum base temperature, (b) average base temperature, and (c) base temperature fluctuations at the applied heat flux of 100 W/cm^2

259×201mm (300×300 DPI)

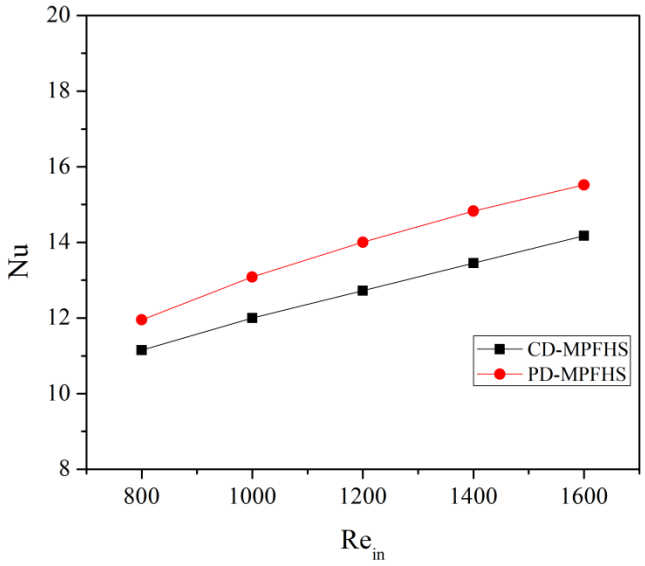

Fig. 9 Comparison of Nusselt number at different Reynolds numbers (Re_{in}) and applied heat flux of 100 W/cm^2

259×201mm (300×300 DPI)

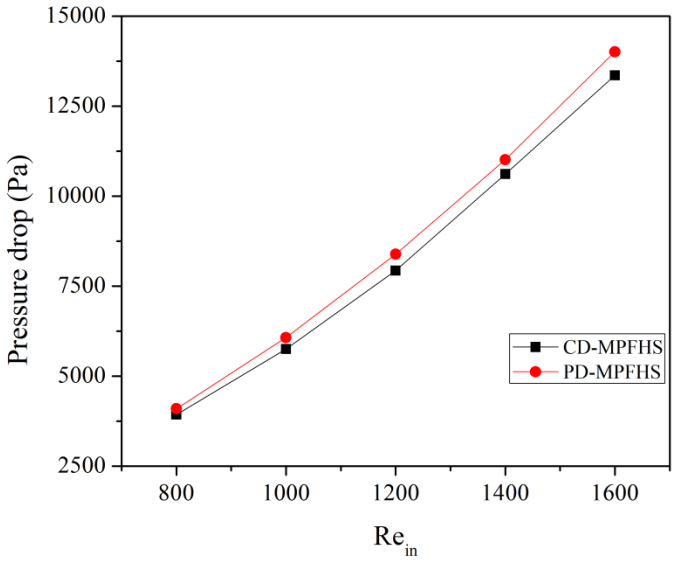

Fig. 10 Comparison of overall pressure drop at different Reynolds numbers (Re_{in}) and applied heat flux of 100 W/cm^2

259×201mm (300×300 DPI)